

Flexible Ti-Ni-N Thin Films Prepared by Magnetron Sputtering

Jindrich Musil, Richard Jílek and Radomír Čerstvý

Department of Physics and New Technologies for Information Society (NTIS), European Centre of Excellence, Faculty of Applied Sciences, University of West Bohemia, CZ-306 14 Plzeň, Czech Republic

Received: December 25, 2013 / Accepted: January 02, 2014 / Published: January 10, 2014.

Abstract: The article reports on flexible Ti-Ni-N films which exhibit an enhanced resistance to cracking in bending. The Ti-Ni-N films were prepared by reactive magnetron sputtering using a dual magnetron. Results of reported experiments demonstrate that: a low effective Young's modulus $E^* = E/(1-\nu^2)$ resulting in a high ratio $H/E^* \geq 0.1$; a high elastic recovery $W_e \geq 60\%$ and a compressive macrostress ($\sigma < 0$) are necessary conditions which ensure that the Ti-Ni-N films exhibit an enhanced resistance against cracking in bending; here E is the Young's modulus and ν is the Poisson's ratio. The Ti-Ni-N films with these properties belong to a new class of advanced coatings called flexible coatings. These coatings are simultaneously hard, tough and resistant to cracking.

Key words: Flexible coatings, hardness, Young's modulus, elastic recovery, macrostress, resistance to cracking.

Nomenclature

H :	Hardness
E^* :	Effective Young's modulus
E :	Young's modulus
W_e :	Elastic recovery
f_r :	Repetition frequency
T :	Pulse period
I_{da} :	Discharge current average of the period
S_{ta} :	Target power density average of the period
S_t :	Target power density
$d_{S,T}$:	Target to substrate distance
U_d :	Discharge voltage
U_S :	Substrate bias
U_{fl} :	Floating potencial
i_S :	Substrate current density
p_T :	Total pressure
p_{N_2} :	Partial pressure of nitrogen
p_{Ar} :	Partial pressure of argon
L :	Indenter load
d :	Diameter of fix cylinder
r :	Radius of fix cylinder

h :	Thickness
a_D :	Deposition rate

Greek Letters

ν :	Poison's ratio
σ :	Macrostress
τ :	Length of magnetron pulse

1. Introduction

Recently, it was shown that the Al-O-N and Zr-Al-O coatings with (1) the low effective Young's modulus $E^* = E/(1-\nu^2)$ satisfying a high ratio $H/E^* \geq 0.1$, (2) the high elastic recovery $W_e \geq 60\%$ and (3) the compressive macrostress ($\sigma < 0$) exhibit an enhanced resistance of film to cracking during its bending [1-4]; here E is the Young's modulus and ν is the Poisson's ratio. The physics behind these properties of the film follows from the Hooke's law $\sigma = E \cdot \varepsilon$; here σ is the stress and ε is the deformation. In the case when the deformation ε of the film material at a given stress σ is required to be increased, the Young's modulus E of material must be decreased. The experiments show that the films with low effective Young's modulus E^*

Corresponding author: Jindrich Musil, Dr.Sc., professor, research fields: physics of thin films, PVD processes, nanocomposite coatings, lasers, plasma physics and propagation of electromagnetic waves in various media. E-mail: musil@kfyz.zcu.cz.

resulting in the high ratio $H/E^* \geq 0.1$ also exhibit high elastic recovery W_e and compressive macrostress σ ; more details are given in Ref. [1].

As this finding could be utilized in many advanced applications, it is necessary to find if also other material systems with properties described above can exhibit an enhanced resistance to cracking. As a next material system in which an enhanced resistance to cracking could be demonstrated we selected Ti-Ni-N coatings. Recently, for instance, it was demonstrated that in the Ti-Ni-N nanocomposite coatings the (200) crystallographic orientation enhances with increasing Ni content [5].

The main aim of this article is a detailed investigation of the structure and mechanical properties of Ti-Ni-N films with low (<10 at.%) Ni content sputtered under different deposition conditions and to assess their resistance to cracking.

2. Experiments

The Ti-Ni-N films were reactively sputtered by a DC pulse and DC dual magnetron with closed magnetic field equipped with Ti/Ni (95/5 at.%) and Ti/Ni (90/10 at.%) targets of diameter $\varnothing = 50$ mm in a mixture Ar + N₂ sputtering gases. The magnetrons were tilted to the vertical axis at the angle 20°; more details in Ref. [6]. The dual magnetron was supplied by an Advanced Energy pulsed power supply at (a) the pulse mode with a repetition frequency $f_r = 100$ kHz, the magnetron discharge current $I_{da} = 2$ A averaged over the pulse period $T = 1/f_r$ and the duty cycle $\tau/T = 0.5$ in bipolar mode and the target power density $S_{ta} = 25$ W/cm² and (b) the DC mode with the magnetron discharge current $I_d = 0.5$ A and the target power density $S_t = 10$ W/cm²; here τ is the length of magnetron pulse. The Ti-Ni-N films were sputtered under the following conditions: substrate-to-target distance $d_{s-t} = 60$ mm, substrate bias U_s ranging from the floating potential U_{fl} to -100 V, substrate ion current density i_s ranging from 0 to ~2 mA/cm², substrate temperature $T_s = 500$ °C, total pressure of the sputtering gas mixture $p_T = p_{N2} + p_{Ar} =$

1 Pa. To improve the adhesion of Ti-Ni-N film to the substrate the TiNi interlayer was inserted between the substrate and the Ti-Ni-N film. The interlayer was sputtered from the Ti/Ni target by a DC dual magnetron at $I_d = 0.5$ A, $U_d = 400$ V, $T_s = 500$ °C, $U_s = 0$ V and $p_T = p_{Ar} = 1$ Pa; here U_d is the magnetron discharge voltage. The Si(100) plates ($20 \times 20 \times 0.3$ mm³ for the X-ray diffraction (XRD) measurements and $30 \times 5 \times 0.3$ mm³ for the macrostress σ measurements) and Mo strips ($80 \times 15 \times 0.1$ mm³ for the assessment of the resistance of film to cracking) were used as substrates.

The film thickness h was measured using a stylus profilometer DEKTAK 8. The macrostress σ was evaluated from the bending of a thin Si plate using the Stoney's formula. The film structure was characterized using an XRD diffractometer PANalytical X Pert PRO in the Bragg-Brentano configuration with CuK α radiation. Mechanical properties were determined from load vs. displacement curves measured by a microhardness tester Fischerscope H100 with a Vicker's diamond indenter at a load $L = 20$ mN. The resistance of the film to cracking was investigated by a bending test. The principle of the bending test is shown in Fig. 1. The Mo strip coated with the Ti-Ni-N film was bended along a fixed cylinder of radius r . A smaller radius r of the fixed cylinder means a higher loading of film and results in its easier cracking.

The formation of cracks in the film was correlated with its mechanical properties. More details are given in Ref. [2]. The Mo strip coated with Ti-Ni-N film was

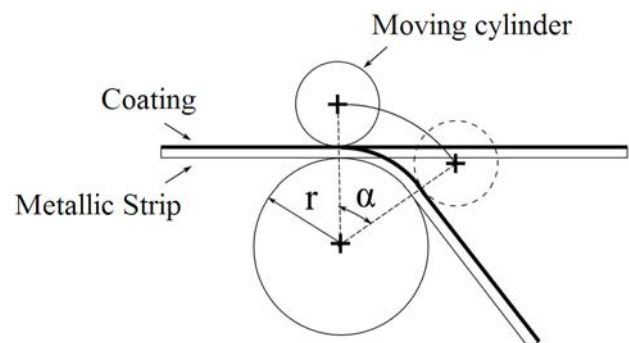


Fig. 1 Schematic illustration of bending test used to create cracks. The Mo strip coated with Ti-Ni-N film is bended along the fixed cylinder of radius r .

bended manually during approximately 3 s up to angle 180° , i.e., with the translation speed around the fixed cylinder of diameter 25 mm of about 12 mm/s.

3. Results and Discussion

It is well known that the properties of the film can be strongly influenced by the energy delivered to it during its growth and by the addition of a selected element in the base material of film [7]. Therefore, the increase of nitrogen N content in film with increasing partial pressure of nitrogen p_{N_2} and the increase of the energy delivered to the growing film with increasing the negative substrate bias U_s were used as main parameters to control the structure and mechanical properties of sputtered Ti-Ni-N films.

3.1 Structure of Ti-Ni-N Films

The evolution of the structure of Ti-Ni-N was investigated as a function of (1) the partial pressure of nitrogen p_{N_2} (Fig. 2) and (2) the substrate bias U_s (Fig. 3). In Fig. 2, it is seen that the structure of Ti-Ni-N film strongly changes with increasing p_{N_2} from a randomly oriented polycrystalline film characterized by TiN(111), TiN(200), TiN(311) and TiN(222) reflections to the film with a strong TiN(220) preferred orientation at $p_{N_2} \geq 0.5$ Pa. The Ti-Ni film prepared in pure argon atmosphere ($p_{N_2} = 0$ Pa) is characterized by strong $-Ti(002)$ reflection and low-intensity reflections of Ti_2Ni phase. The conversion of the randomly oriented polycrystalline film to the film with a strong preferred crystallographic orientation is a result of the competition between the strain and the surface energy in the film. In the TiN crystal, the (200) plane has the lowest surface energy and the (111) plane the lowest strain energy [8]. Moreover, it is known that in the growing film always the crystallographic texture minimizing its total energy is formed. As the increase of compressive macrostress with increasing p_{N_2} is a typical for magnetron sputtered TiN films [9, 10], we believe that the strong (220) preferred orientation formed in Ti-Ni-N films at $p_{N_2} \geq$

0.5 Pa is a result of the competition between the strain and the surface energy in the film, see the decrease of compressive stress in the Ti-Ni-N film deposited at $p_{N_2} = 0.5$ Pa.

In Fig. 3, it is seen that a preferred crystallographic orientation of the Ti-Ni-N film changes from TiN(200) to TiN(111) with increasing negative substrate bias U_s . This change is due to ion bombardment of prepared film which increases the strain energy in film [8]. The evolution of the film structure displayed in Figs. 2 and 3 suggest that the sputtered Ti-Ni-N films are (Ti, Ni)N solid solution nitrides due to a low content of Ni added in the TiN film.

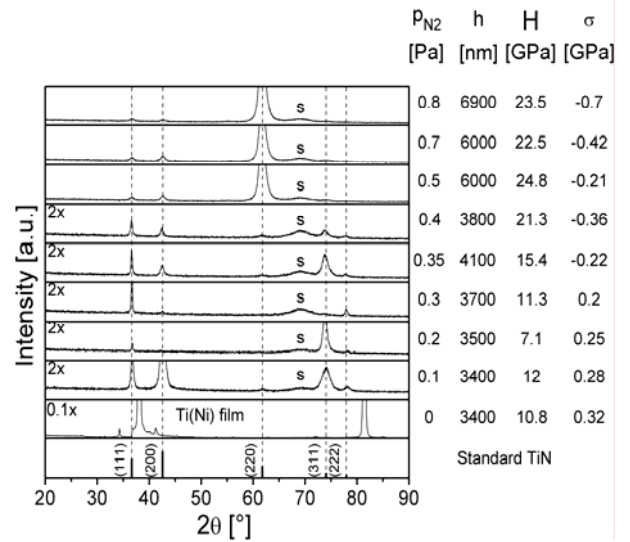


Fig. 2 XRD patterns of Ti-Ni-N film sputtered in pulse bipolar mode from Ti/Ni(95/5 at.%) target at $U_s = U_f$, $T_s = 500$ °C and $p_T = 1$ Pa as a function of partial pressure of nitrogen p_{N_2} .

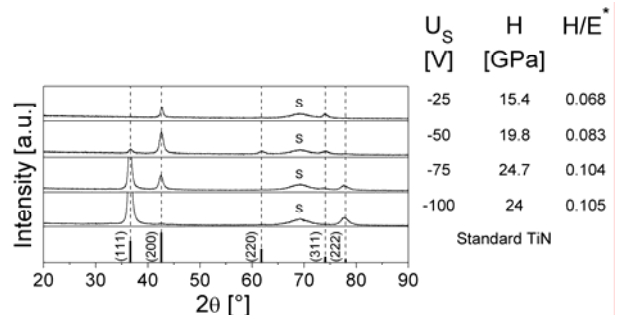


Fig. 3 XRD patterns of Ti-Ni-N films sputtered on Si(100) substrates by DC dual magnetron from Ti/Ni (90/10 at.%) target at $p_{N_2} = 0.8$ Pa, $p_T = 1$ Pa, $T_s = 500$ °C as a function of substrate bias U_s .

3.2 Mechanical Properties and Macrostress of Ti-Ni-N Films

Mechanical properties of the film are the hardness H and the effective Young's modulus E^* . Mechanical behavior of the film is characterized by the elastic recovery W_e , the ratio H/E^* and the ratio H^3/E^{*2} . The ratio H/E^* is proportional to the film toughness [1, 11-14]. The ratio H^3/E^{*2} is proportional to a resistance of the material to plastic deformation [15]. It means that films with enhanced resistance to cracking and plastic deformation should have low values of E^* resulting in high $H/E^* \geq 0.1$ and H^3/E^{*2} ratios. This statement was already confirmed for Zr-Al-O films [2, 4], Al-O-N films [3] and for the Al-Cu-O films [16]. Also, it was found that the films with $H/E^* > 0.1$ are highly elastic ($W_e \geq 60\%$) and exhibit an enhanced resistance to cracking [1-4, 16].

The evolution of the hardness H , effective Young's modulus E^* , elastic recovery W_e , ratio H/E^* and macrostress σ of the Ti-Ni-N films sputtered at $U_s = U_{fl}$, $T_s = 500^\circ\text{C}$ and $p_T = 1\text{ Pa}$ is displayed in Fig. 4. In this figure, it is seen that all films exhibit a low ratio $H/E^* < 0.1$ and a low elastic recovery $W_e \leq 60\%$ but the high hardness $H \approx 21\text{ GPa}$ and the compressive macrostress ($\sigma < 0$) at $p_{N_2} \geq 0.4\text{ Pa}$ and $p_{N_2} > 0.3\text{ Pa}$, respectively. All these films, however, easily cracks because the ratio H/E^* and the values of W_e and compressive macrostress σ are low and thus do not meet necessary conditions needed for the films which should exhibit an enhanced resistance to cracking, i.e., (1) the high ratio $H/E^* \geq 0.1$, (2) the high elastic recovery $W_e \geq 60\%$ and (3) compressive macrostress ($\sigma < 0$) as explained in details in Ref. [1].

Therefore, the Ti-Ni-N films were sputtered under ion bombardment, i.e. at negative substrate bias $U_s < 0$, and at $p_{N_2} = 0.8\text{ Pa}$ when the Ti-Ni-N film sputtered at floating potential ($U_s = U_{fl}$) exhibited the high hardness $H \approx 23\text{ GPa}$ and the low compressive macrostress $\sigma \approx -0.7\text{ GPa}$ and preferred crystallographic orientation TiN(220). Physical and mechanical properties and the macrostress σ of the Ti-Ni-N film sputter deposited

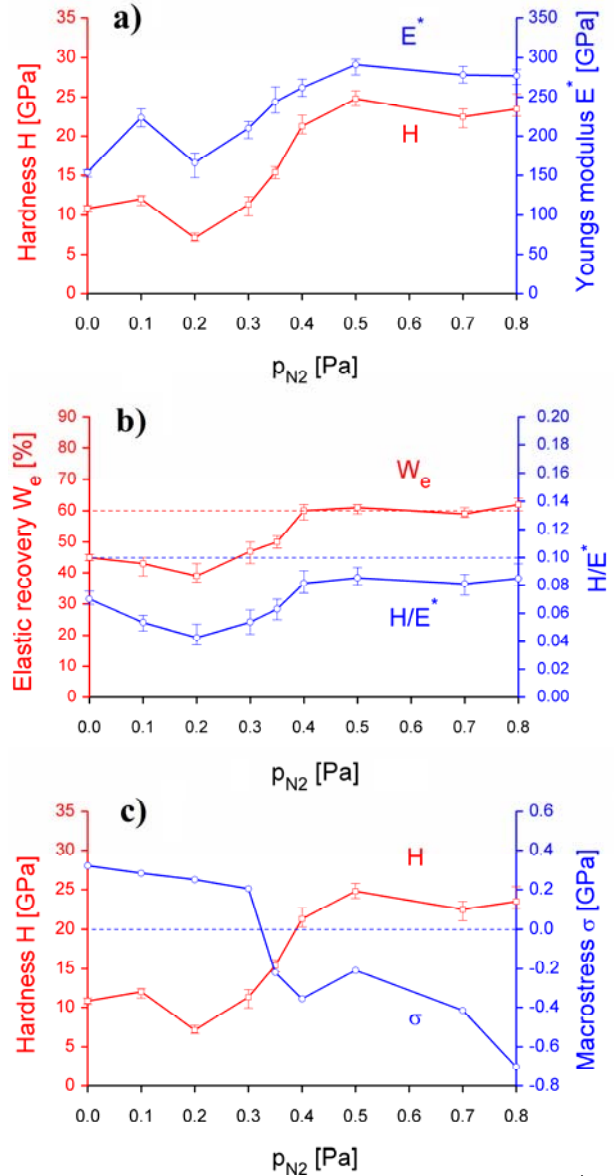


Fig. 4 (a) Hardness H and effective Young's modulus E^* , (b) Elastic recovery W_e and ratio H/E^* , (c) Hardness H and macrostress σ of Ti-Ni-N film sputtered from Ti/Ni(95/5 at.%) target at $U_s = U_{fl}$ as a function of partial pressure of nitrogen p_{N_2} . Measurements were performed at the diamond indenter load $L = 20\text{ mN}$.

under ion bombardment and the conditions under which the film cracks during bending are summarized in Table 1. To apply bias voltage it was necessary to use DC mode and decrease the target power density S_t due to overheating of targets. The increasing negative bias U_s leads to change in crystallographic orientation from TiN(100) to TiN(111) which caused the increase of hardness H , ratio H/E^* and elastic recovery W_e , see

Table 1 Thickness h , deposition rate a_D , hardness H , effective Young's modulus E^* , elastic recovery W_e , ratio H/E^* , macrostress σ of Ti-Ni-N films sputtered by DC dual magnetron from TiNi (90/10 at.%) targets at $p_{N_2} = 0.8$ Pa and different values of substrate bias U_s and i_s on Si(100), Si(100) substrates and Mo strip ($80 \times 10 \times 01$ mm³) without and with TiNi interlayer. H , E^* and W_e were measured by indentation at diamond indenter load $L = 20$ mN.

U_s (V)	i_s (mA/cm ²)	h (nm)	a_D (nm/min)	H (GPa)	E^* (GPa)	W_e (%)	H/E^*	σ (GPa)	Cracks/cylinder of diameter $d = 2r$ (mm)	Film
Ti-Ni-N/Si(100)										
-25	0.7	2,100	16	15.4	228	49	0.068	0.17	yes/25	A
-50	1.8	2,000	15.4	19.8	238	58	0.083	-0.52	yes/15	
-75	2.1	1,800	13.6	24.7	228	71	0.104	-0.46	no/15*	
-100	2.2	2,000	16.7	24	229	67	0.105	-0.31	no/15*	B
Ti-Ni-N/200 nm TiNi/Si(100)										
-75	2.1	1,600	12.3	25.3	244	70	0.104	-1.44	no/10	
Ti-Ni-N/200 nm TiNi/Si(100)										
-100	2.2	1,550	12.9	21.8	197	68	0.111	-1.89	no/10	C

* Ti-Ni-N film was partially delaminated from Mo strip during bending at cylinder of diameter 10 mm.

Table 1. To enhance the adhesion of the Ti-Ni-N film to the substrate the TiNi interlayer was used. The insertion of the TiNi interlayer between the substrate and the Ti-Ni-N film, however, also strongly influences the compressive macrostress σ generated in the Ti-Ni-N film, Table 1. The increase of the compressive macrostress σ in the film is also important for the enhancement of resistance of the Ti-Ni-N film to cracking (Fig. 5 in the Section 3.3). As expected, it was found that the sputter deposition of the Ti-Ni-N film under ion bombardment makes it possible to increase its (1) hardness H , (2) ratio H/E^* above 0.1 and (3) compressive macrostress $|\sigma| > 1$ GPa to values which are necessary to achieve the enhanced resistance of the film to cracking.

3.3 Correlations Between Mechanical Properties, Macrostress and Resistance Against Cracking of Ti-Ni-N Films

The resistance of film to cracking during bending is the higher the smaller is radius r of cylinder along which the coated Mo strip was bended. From Table 1 the correlations between physical and mechanical properties of the film and its resistance to cracking are clearly seen. The Ti-Ni-N films with a low ratio $H/E^* < 0.1$, a low elastic recovery $W_e < 60\%$ and a low compressive macrostress ($|\sigma| < 1$ GPa) easily cracks.

On the other hand, the Ti-Ni-N films with a high ratio $H/E^* \geq 0.1$, a low elastic recovery $W_e \geq 60\%$ and a high compressive macrostress ($|\sigma| \geq 1$ GPa) exhibit an enhanced resistance to cracking. This fact is illustrated in Fig. 4 where the surface morphology of Ti-Ni-N films deposited on Mo strip after bending test is displayed. The film A with low ratio $H/E^* < 0.1$, low elast recovery $W_e < 50\%$ and tensile macrostress σ easily cracks. The film B with high ratio $H/E^* > 0.1$, high $W_e = 67\%$ and low compressive macrostress $\sigma = -0.31$ GPa partially delaminates during bending. On the other hand, the film C with $H/E^* > 0.1$, high $W_e = 67\%$ and high compressive macrostress $\sigma = -1.89$ GPa does not cracks and exhibits an enhanced resistance to cracking as expected. On the other hand crystalpographic orientation TiN(111) exhibit higher surface energy than TiN(100) and TiN(220) [8]. In general the surface energy works against increasing of surface area i.e., the formation of cracks. The higher surface energy of crystalpographic orientation TiN(111) and higher compressive macrostress lead to improvement of the resistance to cracking of the films.

This experiment confirms that the ratio H/E^* , elastic recovery W_e and macrostress σ in the film are main factors influencing its resistance to cracking. The macrostress σ control the crystallographic structure of

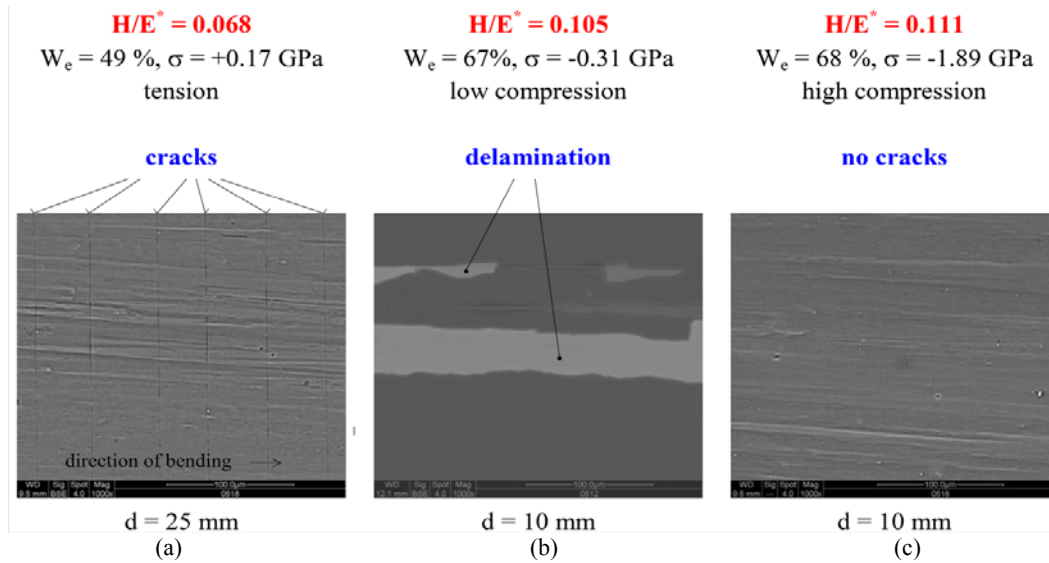


Fig. 5 Surface morphology of Ti-Ni-N film with various (1) macrostress and (2) mechanical properties deposited on Mo strip after its bending along cylinder of diameter $d = 2r$. (a) weakly elastic film with low $H/E^* < 0.1$ in tension (film A), (b) highly elastic film with high $H/E^* > 0.1$ in low compression (film B) and (c) highly elastic film with high $H/E^* > 0.1$ in high compression (film C). Properties of the films A, B and C are given in Table 1.

the film and thus its mechanical properties. Besides, it is necessary to note that the microstructure of film also strongly influences its cracking during bending [1]. The effect of all these parameters on the film resistance to cracking is now under detailed investigation in our labs.

4. Conclusions

The detailed investigation of interrelationships between the mechanical properties of the Ti-Ni-N film and the deposition parameters used in its sputtering showed that

(1) The Ti-Ni-N films sputtered under ion bombardment at negative biases ($|U_s| \geq 75$ V) exhibit the high hardness $H \approx 25$ GPa, high ratio $H/E^* > 0.1$, high elastic recovery $W_e \approx 70\%$ and compressive macrostress ($\sigma < 0$);

(2) The Ti-Ni-N films in compression with high ratio $H/E^* > 0.1$, high elastic recovery $W_e \approx 70\%$ are flexible and exhibit an enhanced resistance to cracking. On other hand, the Ti-Ni-N films in tension ($\sigma > 0$) with low ratio $H/E^* < 0.1$ and low elastic recovery $W_e \leq 60\%$ are brittle and easily crack;

(3) The higher surface energy of crystallographic orientation TiN(111) and higher compressive macrostress increase the resistance of the Ti-Ni-N film to cracking. The correct selection of deposition parameters used in formation of the Ti-Ni-N film is, however, of a key importance for the production of flexible hard Ti-Ni-N films;

(4) The demonstration of the possibility of sputtering of the Ti-Ni-N films with enhanced resistance to cracking indicates that the low effective Young's modulus E^* resulting in high ratio $H/E^* \geq 0.1$, high elastic recovery $W_e \geq 60\%$ and compressive macrostress ($\sigma < 0$) are general necessary conditions which must be fulfilled in case when the flexible films resistant to cracking are required to be formed.

Results of this investigation fully confirm the validity of the conclusions already found for the Al-O-N and Zr-Al-O coatings [2-4].

Acknowledgments

This work was supported in part by the Grant Agency of the Czech Republic under project P 108/12/0393.

References

- [1] J. Musil, Hard nanocomposite coatings: Thermal stability, oxidation resistance and toughness, *Surf. Coat. Technol.* 207 (2012) 50-65.
- [2] J. Musil, J. Sklenka, R. Čerstvý, Transparent Zr-Al-O nanocomposite coatings with enhanced resistance to cracking, *Surf. Coat. Technol.* 206 (2012) 2105-2109.
- [3] J. Musil, M. Meissner, R. Jílek, T. Tolg, R. Čerstvý, Two-phase single layer Al-O-N nanocomposite films with enhanced resistance to cracking, *Surf. Coat. Technol.* 206 (2012) 4230-4234.
- [4] J. Musil, J. Sklenka, R. Čerstvý, T. Suzuki, M. Takahashi, T. Mori, The effect of addition of Al in ZrO₂ thin film on its resistance to cracking, *Surf. Coat. Technol.* 207 (2012) 355-360.
- [5] A. Akbari, J.P. Riviere, C. Templier, E. Le Bourhis, Structural and mechanical properties of IBAD deposited nanocomposite Ti-Ni-N coatings, *Surf. Coat. Technol.* 200 (2006) 6298-6302.
- [6] J. Musil, P. Baroch, Discharge in dual magnetron sputtering system, *IEEE Trans Plasma Science, Part I: Fourth Triennial Special Issue on Images in Plasma Science*, 33 (2) (2005) 338-339.
- [7] J. Musil, Physical and mechanical properties of hard nanocomposite films prepared by reactive magnetron sputtering, *Nanostructured Coatings*, (Chapter 10), Springer New York, 2006, pp. 407-463.
- [8] H.H. Yang, J.H. Je, K.B. Lee, Effect of the nitrogen partial pressure on the preferred orientation of TiN thin films, *J. Appl. Phys.* 79(12) (1996) 9399-9401.
- [9] S. Inoue, T. Ohba, H. Takata, K. Koterayawa, Effect of partial pressure on the internal stress and the crystallographic structure of r. f. reactive sputtered Ti-N films, *Thin Solid Films* 343-344 (1999) 230-233.
- [10] C.A. Carrasco, V. Vergara, R. Benavente, N. Mingolo, J.C. Rios, The relationship between residual stress and process parameters in TiN coatings on copper alloy substrates, *Materials Characterization* 48 (2002) 81-88.
- [11] A. Leyland, A. Matthews, On the significance of the H/E ratio in wear control, a nanocomposite coating approach to optimized tribological behaviour, *Wear* 246 (2000) 1-11.
- [12] A. Leyland, A. Matthews, Design criteria for wear-resistant nanostructured and glassy-metal coatings, *Surf. Coat. Technol.* 177-178 (2004) 317-324.
- [13] A. Matthews, A. Leyland, Material related aspects of nanostructured tribological coatings, in: *SVS Fall Bulletin*, 2008, pp. 40-45.
- [14] J. Musil, J. Jirout, Toughness of hard nanostructured ceramic thin films, *Surf. Coat. Technol.* 201 (2007) 5148-5152.
- [15] T.Y. Tsui, G.M. Pharr, W.C. Oliver, C.S. Bhatia, R.L. White, S. Anders, et al., Nanoindentation and nanoscratching of hard carbon coatings for magnetic disks, *Mater. Res. Soc. Symp. Proc.* 383 (1995) 447-451.
- [16] J. Blažek, J. Musil, P. Stupka, R. Čerstvý, J. Houška, Properties of nanocrystalline Al-Cu-O films reactively sputtered by DC pulse dual magnetron, *Applied Surface Science* 258 (2011) 1762-1767.